

## CALIFORNIA STORM CHARACTERISTICS AND WEATHER MODIFICATION

By Robert D. Elliott

North American Weather Consultants

(Original manuscript received 20 January 1958; revised manuscript received 31 March 1958)

### ABSTRACT

In connection with cloud seeding projects in Pacific Coast states, detailed analyses have been prepared of many storms. From this material, average values of significant parameters have been computed and are employed to construct a model of a typical cold-front-type occlusion moving into the California coast from the west, a type of storm responsible for a substantial fraction of California precipitation.

The model shows some deviations from the classical cold-front-type occlusion, such as the absence of a discernible elevated warm-front surface within 150 mi of the surface cold front. The system is discussed as a steady-state mechanism wherein the generation of liquid moisture in vertical currents is balanced by its removal through precipitation, primarily in the instability zone near the surface front, and by evaporation, primarily in the altostratus zone in advance of the instability zone.

The system being treated as an engine for the production of precipitation reaching the ground, its efficiency is discussed on the basis of simplified calculations of growth of precipitation in relation to ice-forming nuclei supply. It is shown that in this storm model efficiencies are normally well below 100 per cent, and that the introduction of artificial ice-forming nuclei can raise this efficiency markedly.

### 1. Typical storm vertical section

A variety of storm systems approach the California coast from different directions during the October-through-May precipitation season. However, very frequently California and, indeed, the entire west coast of the United States, is affected by extended occlusions whose cyclonic centers fail to cross the coastline but stagnate offshore. In the region several hundred or more miles to the south of these centers the occlusion moves rapidly inland, displaying few warm-front characteristics and behaving more as a strong cold front. It is this sector of the system which contributes most of the precipitation experienced in California.

During the course of cloud-seeding projects in West Coast areas during the past seven years, numerous detailed storm analyses have been prepared. From this material it has been possible to derive average values for significant parameters characterizing the flow pattern, thermal structure, and the distribution of cloud and precipitation for the typical storm system. Fig. 1 depicts the vertical time section normal to the occlusion as it crosses the coastline of California. The abscissa is provided with a distance scale as well as a time scale, based upon an average frontal movement of 25 mph.

The moisture envelope, within which sounding humidities are consistently above 80 per cent, quite likely contains all cloud sheets and cumulus towers. There may also be a number of cloudless layers (between clouds) within this envelope, particularly where the air mass is stable, but on the whole the

envelope can be said to delineate the boundary of cloudy air. The instability envelope contains the region within which there is instability sufficient to bring about deep convective overturning. Within the instability zone, convection cells (or bubbles) are embedded within the general cloud mass. Aloft, in advance of the instability zone, altostratus occurs, with cirrus above and in advance of the altostratus. The lower deck of stratocumulus which thickens as the front approaches is the "deepening marine layer" so characteristic of many West Coast storms. It is the result of lifting of the West Coast inversion and the creation of instability beneath. The air between the altostratus and the stratocumulus is exceptionally dry.

The streamlines depicted by lines and arrows are for the wind in the plane of the section and are relative to the front. Relative horizontal velocities vary from values of 30 mph toward the front in lower levels in advance of the cold front to a similar velocity away from the front in the altostratus zone. The vertical wind component has been computed by application of the continuity equation and is found to range mostly between 10 and 15  $\text{cm sec}^{-1}$  in the instability zone, and about 5  $\text{cm sec}^{-1}$  in the altostratus zone.

The isotherms are based upon average soundings and considerations of horizontal and vertical advection, and of convection. The air is first lifted along the streamlines wet adiabatically as it moves toward the front (or the front moves toward it with reference to the earth). In the course of approaching the front, however, the situation arises that the air column becomes steadily warmer at lower levels. This is due to

the strong low-level horizontal advection of warm air in the increasing southerly flow just in advance of the front. This factor alone can lead to instability and to convective overturning. Hence there is some warming aloft due to convective transport of heat upward. As the deep moist-air stream approaching the front rises, the potentially warmer air lies to the left, the colder to the right. This air stream itself "overturns" as it moves out in advance of the front in the stronger flow aloft (in the altostratus zone). Thus the potentially warmer air comes to the top, and the air stream is stabilized. However, this process is partly counterbalanced by convective mixing and does not account fully for the strong stability observed in the altostratus zone. Apparently the slight stability of the

entering air stream is amplified by shrinkage of the vertical column as a result of high-level lateral spreading in the direction normal to the cross-section plane, and longitudinal stretching when stronger winds are attained at higher levels downwind. The stabilizing action takes the form of the development of a number of stable layers, or inversions, and the layering of cloud forms.

The air between the upper- and lower-air stream (the altostratus and stratocumulus decks) is stable as well as dry. It is the air which normally exists above the West Coast inversion and its stability is reduced little, if at all, by the motion it undergoes. Rain or snow falling from the altostratus seldom penetrates visibly more than 1000 ft. Precipitation, as indicated

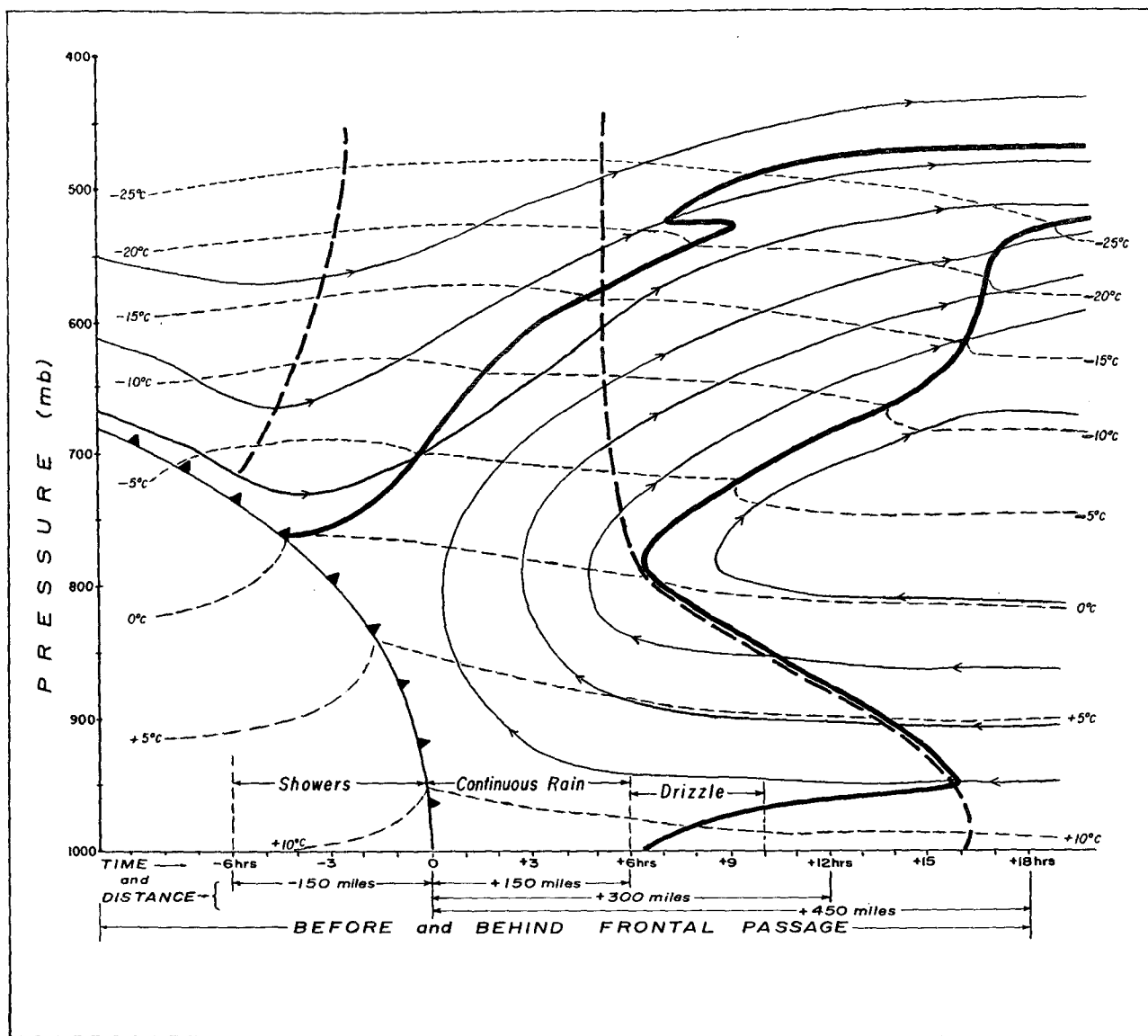


FIG. 1. Typical vertical section normal to the cold front. The abscissa scale refers to hours before (+) and hours after (-) frontal passage and to distance ahead of (+) and distance behind (-) the surface front. The solid line envelopes a region possessing over 80 per cent relative humidity. The dashed line envelopes a region of instability. Air motion relative to the front is indicated by arrows. Dotted lines are isotherms.

in the section, reaches the ground in appreciable quantity only where there is no dry zone remaining.

Although there is usually at least one inversion of moderate intensity near the base of the upper-air stream, there is no evidence of any inversion or stable layer, much less a well marked "warm front" aloft, within 6 hr of frontal passage. The system is, by its synoptic development, classifiable as cold-front-type occlusion, but it fails to exhibit the warm-front temperature discontinuity of the classical model near the surface front.

A most interesting feature of the cross section is the manner in which the top of the moisture envelope descends as the front is approached. Although the altostratus deck attains low enough temperatures for intensive natural nucleation to occur, the highest point achieved by the unstable clouds averages about  $-15^{\circ}\text{C}$ . The superior air descending over the cold front appears to force the cloud top down even though the air mass is unstable above cloud top level. Penetrative convection undoubtedly transports some moisture into the superior air mass so that there is a rising boundary layer and some superior-air streamlines enter the moisture envelope. Pilot reports indicate bulging cumulus tops sometimes rise above the general cloud mass in this region. Farther downwind the superior air is lifted sufficiently for sublimation to occur and cirrus to form, as indicated in the cross section.

Precipitation from the marine deck in advance of the instability zone is generally of a drizzle type, although none may fall in some cases. At the boundary of the instability zone there is a sudden increase in precipitation intensity with moderate intensities developing in sometimes as little as a few minutes. In the case where the marine deck is not present, precipitation commences suddenly when the altostratus base falls to about 6000 ft. By then the base of the altostratus is apparently at the top of the moist, but not fully saturated, marine layer. Saturation occurs quickly and a lower stratocumulus deck develops, merging soon in the general cloud mass of the instability zone. Moderate-intensity precipitation continues for 3 or 4 hr, then tapers off to light. It may entirely cease before passage of the surface front. Post-frontal instability showers are not discussed in this paper.

Rainfall records obtained by means of recording gauges exhibit a certain degree of intensity pulsation within the instability zone. The period between peaks averages approximately 20 min. At first, the 3-cm PPI radar-scope echoes show a rather soft appearance in this zone but nevertheless some pattern is discernible, with sharper echoes developing as the cold front nears. It seems likely that, as the low-level warm-air advection from the south proceeds, a slightly superadiabatic lapse rate develops in the lower levels, leading to the

development of convective bubbles or cells having a total updraft area small enough compared to the exterior area that compensating exterior subsidence is smaller than the general ascending motion in the instability zone. Thus the exterior zone remains saturated and evaporation is not an important factor there.

The rising convection bubbles and chimneys are subject to considerable vertical shear within the instability zone, and are therefore tilted, and may also be completely torn asunder. The chance of attaining liquid-water contents approaching those of the wet adiabatic ascent value is diminished by these processes, but the depletion of the liquid-water content by the generally continuous precipitation in this zone is by far the more important factor in preventing adiabatic accumulation of water. The depletion is proportional to liquid-water content and the water content is therefore brought down rapidly to values in line with those in the exterior area. It is believed that the distribution of liquid moisture within the instability zone averages close to that due to the slow lifting and condensation in the ascending air stream after taking into account the steady depletion by precipitation.

The dimensions and other physical characteristics of the storm section are average values based primarily upon two winter seasons of four-times-a-day rasonde observations at Oakland and one at Santa Monica. There can be significant variations from these averages; however, there is some correlation between these variations. For instance, the deeper the storm (the higher the highest point within the instability zone) the colder the cloud-top temperature, and the stronger the outflow wind there. Also, the deeper the storm, the greater its lateral dimension, although this relationship is not linear.

The storm section depicts a steady-state condition of wind, temperature, cloud, and precipitation distribution relative to frontal position. Liquid water in the form of cloud droplets is generated in the updrafts through condensation. Growth of precipitation-size particles through sublimation is most active at cloud-top level in the instability zone and in the altostratus zone. Upon descent through the sub-freezing cloud layer, growth continues as liquid and solid matter are accreted. At above-freezing temperatures the falling raindrops grow by coalescence as they scour out the cloud droplets. The depletion of the cloud water content by accretion and coalescence provides the mechanism whereby liquid-water contents are maintained far below the adiabatic ascent value.

The "scouring" efficiency of precipitation elements in general depends upon their collection efficiency, the cross-sectional area of the particle, and the liquid-water content of the cloud being swept out. Thus, precipitation limits its own effectiveness by depletion of the liquid-water "reservoir" held in the cloud.

Under steady-state conditions, the precipitation-particle size plays the dominant role, so that the permissible reservoir of liquid water is greatest at high levels where the precipitation elements are still quite small. In the zone where tops are low and sublimation inefficient, precipitation may be initiated first by the larger cloud droplets acting in the condensation-coalescence process, as has been outlined by East (1957). However, the prior initiation by this process depends upon cloud-base temperature as shown by MacCready (1956) and the required temperatures are usually not attained.

Within the storm system there exist gradients of liquid-water content along which both the horizontal and vertical wind components blow. There is an important advection of water outward from the top of the instability zone into the altostratus zone. Although the net evaporation in the zone of heavier precipitation is small, evaporative loss of potential precipitation in this altostratus zone in this type of storm is almost complete, being either lost as the virga evaporates into the dry layer beneath the altostratus (which is being transported away from the front), or lost when the higher clouds slowly evaporate over the cold dome.

If the storm is conceived of as an engine for converting the liquid water it generates into precipitation reaching the ground, then its efficiency in performing this operation can be evaluated. If  $G$  represents the rate of generation of total liquid or solid water in the form of cloud elements,  $P$  represents the rate of total precipitation in any form reaching the ground, and  $E$  represents the rate of total evaporation, then the storm efficiency is defined as:

$$e = \frac{P}{G} = \frac{G - E}{G}. \quad (1)$$

If the term  $E$  is omitted, as was done by Weickmann (1957) in his general discussion of efficiency, then the efficiency is 1.0 which implies that variations in supply of ice-forming nuclei or other precipitation-forming particles have no effect on efficiency.

It is convenient for the sake of discussion to employ the two major storm divisions: the instability zone and the altostratus zone. If we disregard, for the time being, the transport of liquid water into the instability zone in the low-level marine layer, then the net transport  $T$  from the instability zone into the altostratus zone equals  $E$  (on the assumption of total loss in the altostratus zone) and the efficiency is:

$$e = \frac{G - T}{G}. \quad (2)$$

In order to compute the efficiency of the storm, it is necessary to know the distribution of cloud water

content. As far as direct observations are concerned, this is unknown. Published values for nimbus by aufm Kampe (1957) indicate less than  $0.5 \text{ gm m}^{-3}$  is most common. On the other hand, the presence of strong vertical motion in this system, in contrast to that of typical warm-frontal altostratus or nimbostratus, argues for a higher value. If we assume an average of  $0.75 \text{ gm m}^{-3}$ , with a mean outflow of  $15 \text{ m sec}^{-1}$  across the zone boundary and an outflow depth of  $2.3 \text{ km}$  on top of a base layer of  $2.3 \text{ km}$ , then the total water-loss rate in a one-centimeter-wide strip is  $258 \text{ grams cm}^{-1} \text{ sec}^{-1}$ . The water generated within the instability zone, or in the marine deck and transported therefrom into the instability zone, is equivalent to that which would be observed under conditions of adiabatic ascent, with no depletion through precipitation. Under these conditions, the average concentration in the top  $2.3\text{-km-thick}$  layer would be approximately  $5.1 \text{ gm m}^{-3}$ . This is being replaced as fast as it is being transported out into the altostratus zone. Therefore,  $G$  is equal to  $17.6 \cdot 10^2 \text{ gm cm}^{-1} \text{ sec}^{-1}$  and the efficiency is 0.85. In storms where the sub-altostratus layer is so moist that some precipitation reaches the ground, higher efficiencies prevail. On the other hand, it seems clear that where the cloud tops in the instability zone are at relatively warm temperatures, nucleation will be inefficient and a sizeable reservoir of liquid droplets accumulates to be transported outward and lost eventually by evaporation. Here efficiencies may be considerably lower than 0.85.

## 2. Discussion of role of ice-forming nuclei supply in generation of precipitation

In order to demonstrate the importance of nuclei supply in the efficiency of this type of storm, some calculations based upon a simplified model have been made. Let us consider first the growth processes of sublimation and accretion. At the top of the cloud, sublimation leads to rapid growth of ice crystals. With the liquid-water contents, which we shall be dealing, growth by accretion will be important so that graupel and ice pellets soon appear. After melting develops at lower levels, the raindrops grow by collision and coalescence.

Douglas (1957) has treated in considerable detail growth by sublimation and by accretion. In altostratus possessing a liquid water content of  $1.0 \text{ gm m}^{-3}$ , he found growth by accretion becomes as important as that by sublimation at  $200\text{-}\mu$  melted radius. Houghton (1950) had estimated that this occurred at about  $130\text{-}\mu$  radius. Douglas compares his computed growth rates by sublimation and accretion of spherical particles of widely varying densities and different cloud liquid-water contents to growth rates of a droplet by coalescence. It appears that beyond  $100\text{-}\mu$  melted

radius the growth of liquid droplets and of ice spheres is nearly the same. Growth to this size is quite rapid, thanks primarily to sublimation, and occurs in approximately 10 min. This means that under the conditions with which we are concerned, an assumed rapid growth to 100- $\mu$ -radius spheres in the top fraction of a kilometer is reasonable.

We shall employ as a simplified model a 4.6-km-deep column of cloud in which the generation of liquid moisture by condensation occurs in a uniform updraft. The depth is measured downward from the level  $z=0$ , at which point 100- $\mu$ -radius ice spheres of density 1 are introduced, having been formed in the thin layer of cloud above  $z=0$ . Below the cloud base, convergence occurs to provide the constant upward vertical motion in the column. We shall be dealing with a constant-precipitation-element size and a constant-cloud-element size at any given level.

The ice spheres (or raindrops) will fall downward and grow by collision and coalescence. The rate of volume growth at a given height depends upon the area swept out by the falling particle or drop and the liquid-water content of the atmosphere, in the following manner:

$$d\left(\frac{4}{3}\pi r^3\right) = E\pi r^2 w V_i \cdot dt \cdot 10^{-6}, \quad (3)$$

where  $E$  is the collection efficiency,  $r$  is the particle radius,  $w$  is the liquid-water content in grams per cubic meter,  $V_i$  is the terminal velocity, and  $dt$  is the time increment. In the mild mean up-current of this model, we shall assume  $V_i dt = dz$ ,  $dz$  being the incremental distance of fall. Thus,

$$dr = \frac{E}{4} w dz \cdot 10^{-6}. \quad (4)$$

The weight of liquid water removed at depth  $z$  by a single particle or drop is then

$$dm = 4\pi r^2 dr = E\pi r w dz \cdot 10^{-6}. \quad (5)$$

The flux of ice particles into the top of the column is

$$F = NV_i \cdot 10^{-6}, \quad (6)$$

where  $V_i$  is the velocity with which fresh nuclei are supplied from below to replace those which are being precipitated out. It is clear that with a constant vertical velocity  $V_z$ ,  $V_i = V_z$ . The value of  $N$  is essentially the number of nuclei per cubic meter in the free atmosphere which are effective at sublimation-level temperature.

The time rate of depletion of liquid water at any depth  $z$  due to precipitation growth per unit volume at that level can be computed from (5) and (6):

$$dM = Fdm = NV_z \pi r^2 E w dz \cdot 10^{-12}. \quad (7)$$

The complete water balance equation in the column is

$$\frac{dw}{dt} \cdot 10^{-6} = V_z \frac{\partial w}{\partial z} \cdot 10^{-6} = -dM + G \quad (8)$$

where  $G$  is the rate of generation of liquid water per unit volume by adiabatic ascent. To simplify computations, it is assumed  $G = KV_z$ . The value for  $K$  does not vary greatly from its average of  $1.5 \cdot 10^{-11}$  in the range of altitudes of concern. Horizontal transport of water will be considered only in the final estimate of efficiency.

The collection efficiency  $E$  depends primarily upon cloud-droplet size but also on precipitation-drop size, according to Langmuir's (1948) treatment. It is therefore desirable to know not only  $r$ , but also  $r_{cd}$ , the cloud-drop diameter. Howell (1949) has determined that condensation results in a rapid growth of cloud droplets to 10- $\mu$  size. However, where  $r$  is large, growth of  $r_{cd}$  to even this size may be inhibited and, hence,  $E$  materially reduced. East (1957) has treated the change in spectrum with further condensation to high liquid-water contents. The peak value in his spectrum shows an increase such as one would expect basically with further condensation upon the original cloud droplets assuming a monodisperse cloud with  $\bar{r}_{cd}$  = the peak value; *i.e.*, it might be assumed that the mean-droplet radius depends upon the cube root of the liquid-water content. This assumption has been made in these computations.

Equations (7) and (8) are combined, giving:

$$\frac{\partial w}{\partial z} = -N\pi r^2 E w \cdot 10^{-6} + 1.5 \cdot 10^{-11}. \quad (9)$$

Equations (4) and (9) can be solved jointly for various values of  $N$  by numerical process. This provides us with the equilibrium vertical distribution of  $w$  for various values of  $N$ . The mean value of  $w$  in the top 2.3 km of the column is then computed and equation (2) employed to estimate the efficiency.

Fig. 2 portrays values of efficiency for various  $N$ ; cloud top values for  $w$  are also shown. The temperatures appearing on the bottom scale are those most frequently found associated with the corresponding  $N$  values in samplings of natural-nuclei concentrations by Bigg (1955), Smith *et al* (1956), MacCready, (1957), and by the author in California. There has been considerable speculation on the spatial and temporal variations in the value of  $N$ ; however, as observations have accumulated, it appears that at least some of the suspected variability was the result of variations in observing techniques. Recent comparison tests reported on by MacCready (1957) show the extent to which different observing techniques vary in their determinations of  $N$ .

It is seen that successive order-of-magnitude increases in  $N$  lead to a considerable but diminishing increase in efficiency. It is important to note here that with a greater value of  $N$ , although somewhat heavier precipitation occurs, the final raindrop size is smaller. This results from the sharing of the available water by so many more nuclei.

If snow crystals in the form of spatial aggregates of dendrites or plates are as effective collectors as Weickmann (1957) claims, then it would appear that efficiencies are higher than those computed, for cloud top temperatures in the  $-20\text{C}$  to  $-25\text{C}$  range. Other factors omitted in this simplified analysis may also increase or decrease the computed efficiency, and the information appearing in fig. 2 can be considered only as an approximate indication of the effect of variations in nuclei supply on efficiency. In particular, the computation of the vertical distribution of  $w$  ignores the effect of horizontal transport of water into or out of the column. It is seen that, in the lower levels, undepleted and therefore high liquid-water-content air moves, in a relative sense, into the precipitation zone. This will intensify precipitation over the computed value until the liquid-water content is reduced to the computed steady-state value. Closer to the front, the warmer cloud-top temperature, and consequently smaller number of effective nuclei, results in a decrease in rainfall intensity. For this reason, the liquid-moisture reservoir increases and, as the air rises and

moves away from the front, it again enters the heaviest-precipitation zone with a liquid-moisture content in excess of the computed steady-state condition. Convective mixing, of course, tends to equalize these differences.

In the region of warmer cloud tops, the condensation-coalescence process can provide growth particles in concentrations of  $10^2 \text{ m}^{-3}$  according to Ludlam (1956). Under steady-state conditions, the liquid-water content at cloud top would be less than that shown in fig. 1 for  $N=10^2$  because of a smaller depth, but it might still be sufficient for precipitation initiation by condensation-coalescence. However, with only  $10^2 \text{ m}^{-3}$  trigger particles available, the overall efficiency under a steady-state condition would not be great.

### 3. Artificial nuclei supply

The preceding discussion serves to highlight the important role which nuclei supply plays in governing the efficiency of this type of a storm system. It is clear that efficiency can be increased if nuclei supply can be enhanced artificially. That this is possible is suggested by the following considerations.

The effective source strength of a silver-iodide smoke generator varies with the temperature at which the nucleation occurs, according to MacCready (1956) and others. Thus, a typical propane type generator emits approximately  $10^{13}$  nuclei per second effective

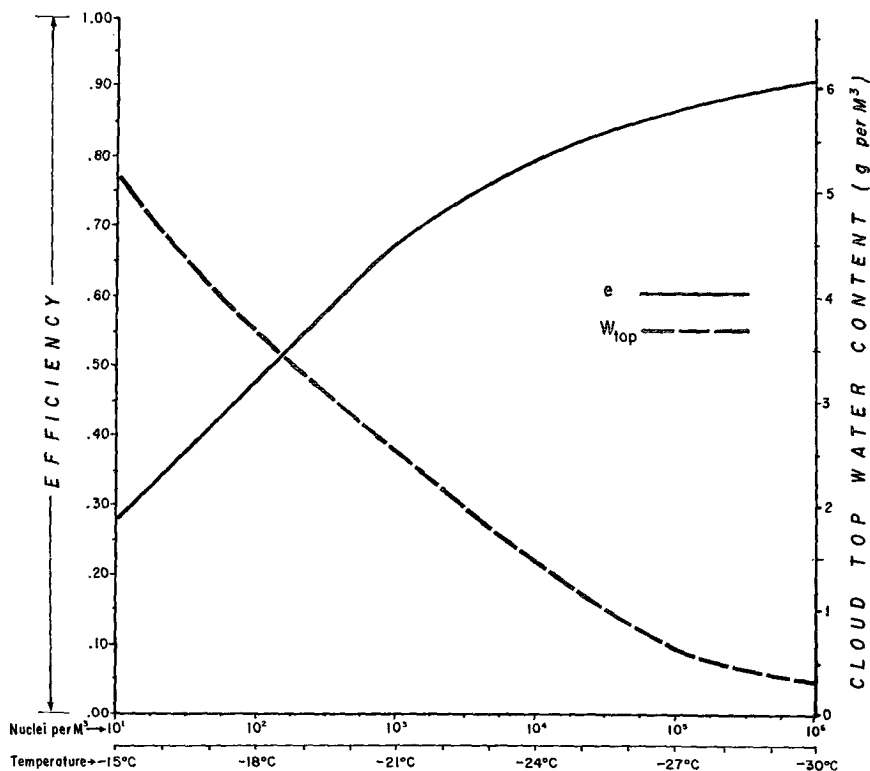


FIG. 2. Computed efficiency and cloud-top water content vs. nuclei concentration.

at  $-20^{\circ}\text{C}$ ,  $2 \times 10^{12}$  effective at  $15^{\circ}\text{C}$ , and  $10^{10}$  effective at  $-10^{\circ}\text{C}$ . Suppose the entire smoke production of one generator is entrained in one large convection cell of  $10 \text{ km}^2$  cross section possessing a mean updraft of  $2.5 \text{ m sec}^{-1}$ . The computed concentration of nuclei at various temperatures, and the ratio of this artificial concentration to average natural-background concentration, appears in table 1. The natural-background nuclei concentrations are those employed in fig. 2.

TABLE 1. Comparisons of artificial and background nuclei concentrations.

Temp. (C)	AgI Nuclei conc. No. per $\text{M}^3$	Background conc. No. per $\text{M}^3$	Ratio $\frac{\text{Artificial}}{\text{Background}}$
-30	$10^7$	$10^6$	10
-25	$2 \times 10^6$	$2 \times 10^4$	$10^2$
-20	$4 \times 10^6$	$5 \times 10^2$	$8 \times 10^2$
-15	$8 \times 10^4$	$10^1$	$8 \times 10^3$
-10	$4 \times 10^2$	$2 \times 10^{-1}$	$2 \times 10^3$

These computations have been made under the assumption of no photolytic decay. Recent field studies (MacCready *et al.*, 1958) of nuclei concentrations downwind from ground-based generators emitting silver-iodide smoke in bright summer daylight have indicated decay rates of half an order of magnitude per hour. The cell here considered involves times of exposure of approximately half an hour with little light during the day and none at night. A minor and uncertain correction for this factor was therefore not made. The effectiveness of convective activity in distributing the smoke throughout the cloud region was also demonstrated in this same field study.

According to table 1, the artificial-nuclei count exceeds background count over a wide range of temperature by 2 to 4 orders of magnitude. The probable enhancement of nuclei concentrations over a wide range of temperatures, while recognized, has not been given as much consideration in the theory of seeding as has the lowering of the threshold level of nucleation. Under the conditions of broadscale entrainment and lateral mixing with which we are concerned, and assuming a reasonably spaced network of continuously operated generators, it is likely that an average concentration of 10 to  $10^2$  that of background can be maintained.

According to the discussion of fig. 2, it appears reasonable to expect a considerable increase in storm efficiency with this nuclei enhancement where the cloud top is at  $-15^{\circ}\text{C}$ . From this viewpoint, the effect of cloud seeding is not merely a matter of releasing a part of the existing reservoir of liquid water, as has been proposed by Weickmann (1957) in connection with stable warm-front precipitation, but rather is a matter of changing the steady-state condition so as to increase overall efficiency.

This view can be extended to the analysis of a range of precipitation generating systems. Braham's (1952) figures for the water budget of the thunderstorm indicate a measured 19 per cent efficiency for that system. It seems likely that an extended and stable warm front, on the other hand, would have a very high efficiency provided the sub-Ast layers were moist. It is to be noted, however, that the mechanism generating the liquid moisture in all systems is the updraft or upslope motion and that this mechanism produces liquid water at the slowest rate in the most efficient system—namely, the warm front; and it produces liquid water at the fastest rate in the least efficient system—the thunderstorm. Thus, for all its inefficiency, an area of thunderstorms produces much more precipitation than does a stable-type warm front. In general, we should expect the artificial enhancement of nuclei supply to provide greatest increases in efficiency in the case of the naturally-low-efficiency systems.

Additionally, it should be emphasized that the most profound effect of artificial-nuclei enhancement is the increase in the number of precipitating elements. This, of course, leads to a decrease in their size. In purely convective situations it is possible to increase nuclei concentrations over background values by  $10^3$ , which might lead to a tenfold reduction in precipitation-element size.

The effect of topography on the storm system is twofold. Vertical velocities are increased on upwind slopes, thus greatly increasing the rate of generation of water there, and the release of convective instability is also much increased. The latter is a factor of great importance to the seeding of upwind mountain slopes, particularly where the crest is below nucleation level. The treatments of continuous seeding in orographic situations by Bergeron (1949) and Ludlam (1956) consider only the case where the crest is in the nucleation zone.

#### 4. Conclusions

From the foregoing, it appears that the efficiency of the storm section depicted by fig. 1 in converting the liquid moisture it generates into precipitation depends primarily upon the rate of supply of ice-forming nuclei. The precise computation of this effect is not attempted, primarily by reason of the complex pattern of interacting processes involved. The simplified computations performed indicate that artificial enhancement of ice-forming nuclei supply with existing silver-iodide smoke generating equipment can increase efficiencies and, therefore, rate of precipitation by a significant amount.

The direct sampling of the water distribution in liquid and solid form in a number of storms would, along with conventional synoptic data, provide a much

better basis for the computations of the various terms of the efficiency equation.

The section depicted by fig. 1 is typical of the storm type responsible for a substantial fraction of precipitation received in California—namely, an extended cold-front-type occlusion south of a cyclonic center stagnating off the coast of the Pacific Northwest. A more complicated analysis would be required to compute efficiencies in storms where appreciable precipitation reached ground level from the altostratus zone. It must not be inferred that the model presented is typical of all California storms.

It should also be pointed out that no consideration has been given to the dynamic effects of increased buoyancy resulting from artificially initiated nucleation at lower levels. It has been demonstrated by Battan and Kassander (1958) that seeding raises the tops of convective cumulus.

Finally, it is suggested that inasmuch as the nuclei supply is the one variable in the atmospheric outdoor laboratory over which man possesses a modicum of control, he can effectively increase his knowledge of cloud physics and the precipitation process by controlling this variable, and observing and interpreting results.

*Acknowledgements.*—The author is indebted to Rear Admiral F. A. Berry, USN (Ret.), and Raymond E. Kerr, Jr., for their review of this paper and their helpful suggestions, and to Jean L. d'Argastel for the drafting of the figures.

#### REFERENCES

- aufm Kampe, H. J., and H. K. Weickmann, 1957: Physics of clouds. *Meteor. Monogr.*, **3**, 182–225.
- Battan, L. J., and A. R. Kassander, Jr., 1958: *Design and execution of a program of randomized seeding of orographic cumulus*. Pap. presented at 163rd Natl. Meet. Amer. meteor. Soc.
- Bergeron, T., 1949: The problem of artificial control of rainfall on the globe. *Tellus*, **1**, 1.
- Bigg, E. K., 1955: Ice-crystal counts and the freezing of water drops. *Quart. J. r. meteor. Soc.*, **81**, 478–479.
- Braham, R. R., Jr., 1952: The water and energy budgets of the thunderstorm and their relation to thunderstorm development. *J. Meteor.*, **9**, 227–242.
- Douglas, R. H., Jr., 1957: *Growth of precipitation elements by sublimation and accretion*. Sci. Rep. MW-26, McGill Univ. MacDonald Phys. Lab. "Stormy Weather" Res. Group.
- East, T. W. R., 1957: A precipitation mechanism in cumulus. *Quart. J. r. meteor. Soc.*, **83**, 61–75.
- Houghton, H. G., 1950: A preliminary quantitative analysis of precipitation mechanisms. *J. Meteor.*, **7**, 363–369.
- Howell, W. E., 1949: The growth of cloud drops in uniformly cooled air. *J. r. meteor. Soc.*, **6**, 134–149.
- Langmuir, I., 1948: The production of rain by chain reaction in cumulus clouds at temperatures above freezing. *J. Meteor.*, **5**, 175–192.
- Ludlam, F. H., and P. M. Saunders, 1956: Shower formation in large cumulus. *Tellus*, **4**, 424–442.
- , 1956: Artificial snowfall from mountain clouds. *Tellus*, **3**, 277–289.
- MacCready, P. B., T. B. Smith, C. J. Todd, and K. M. Beesmer, 1956: *Physical evaluation of cloud seeding effects*. Pasadena, Meteor. Res., Inc., 43 pp.
- , 1957: *Report on the Pasadena cooperative program of ice nuclei measuring techniques to advisory committee on weather control*. Pasadena, Meteor. Res., Inc.
- , 1958: *Nuclei, cumulus, and seedability studies*. Final Rep., Advis. Comm. on Wea. Control, **2**, 185–190.
- Smith, E. J., A. R. Kassander, and S. Twomey, 1956: Measurements of natural freezing nuclei at high altitudes. *Nature*, **177**, 82–83.
- Weickmann, H. K., 1957: Physics of precipitation. *Meteor. Monogr.*, **3**, 226–255.